Tunable clover-shaped GaN photonic bandgap structures patterned by dual-step nanosphere lithography

K. H. Li, Zetao Ma, and H. W. Choi[a)]
Department of Electrical and Electronic Engineering, The University of Hong Kong, Hong Kong

(Received 17 January 2012; accepted 13 March 2012; published online 2 April 2012)

The fabrication of close-packed clover-shaped photonic crystal structure on GaN by dual-step nanosphere lithography is demonstrated. By shrinkage of spheres prior to pattern transfer, a non-closed-packed clover-shaped photonic bandgap (PBG) structure, as designed by modified 3D finite-difference time-domain simulation, is also realized. The PBG of the close-packed and non-close-packed clover-shaped structures is verified through optical transmission spectroscopy, found to agree well with simulated results. A threefold enhancement in photoluminescence (PL) intensity is observed from the optimized structure, when the PBG is tuned to overlap with the emission band of the InGaN/GaN multi-quantum wells. From time-resolved PL measurements, shortened decay lifetimes are observed. © *2012 American Institute of Physics*. [http://dx.doi.org/10.1063/1.3698392]

Photonic crystals (PhCs), with unique capabilities of being able to control and manipulate the propagation of light, have been widely adopted in diverse optoelectronic and photonic applications, including laser resonant cavities,[1] high-speed optical fiber transmission,[2] and polarization filtering.[3] The incorporation of two-dimensional (2D) PhCs onto the surfaces of nitride-based light-emitting diodes (LEDs) has also been demonstrated to effectively promote light extraction efficiency.[4,5] Such ordered periodic nanostructures, with the ability of manipulating spontaneous emission, can be extremely useful for extracting guided modes to air, thus enlarging the escape cone. With a well-defined periodic arrangement and with sufficiently large refractive index contrast between GaN and ambient, a photonic bandgap (PBG) may be established, which forbids the propagation of light within a specific range of frequencies dependent on the dimension and pitch of the array. The PBG can thus be exploited for suppressing lateral wave-guiding and possibly redirect a significant proportion of trapped photons for extraction, overcoming one of the major limitations of nitride LEDs. Traditionally, the formation of two-dimensional PBG structure relies heavily on high-precision direct-write electron-beam lithography,[4] but low-throughput and high equipment cost make this impractical for large-scale fabrication. Nanosphere lithography (NSL) has emerged as a practical approach for patterning large-area ordered periodic nanostructures. NSL overcomes resolution issues arising from diffraction limit in optical lithography and even beam size limitations in e-beam lithography. Nanosphere array can simply be coated by spin-coating or vertical deposition, producing two-dimensional closed-packed hexagonal monolayer. The self-assembled sphere array then serves as an etch mask for pattern transfer to form periodic arrays of recessed air-holes or protruding pillars. However, close-packed nanostructures do not provide a suitable periodic variation of refractive index in the lateral direction so that a PBG corresponding to transverse electric (TE)-dominated emission from InGaN/GaN multi-quantum wells (MQWs) does not exist. From our prior works, various nanosphere-patterned PBG structures in the visible spectral regions have been demonstrated, including the hemi-ellipsoidal geometry[6] and air-spaced nano-pillars.[7]

The work being presented here adopts a dual-step NSL for generating close-packed (CP) clover-shaped PhC structures. It can also be extended to pattern non-closed-packed (NCP) clover-shaped structures through an additional dimension-adjusting process. By adjusting the air spacing, the PBG position can be tuned to spectrally overlap with the emission band of InGaN/GaN MQWs. Transmission measurement is carried out to locate the position of the PBG, which is found to correlate well with 3D-finite-difference time-domain (FDTD) simulated results. The effects of having a PBG on light extraction and recombination decay lifetime are also discussed.

Fig. 1 illustrates the process flow for fabricating a clover-shaped PhC structure. The metal-organic chemical vapor deposition (MOCVD) grown InGaN/GaN MQW LED on c-plane sapphire substrate emits at center wavelength of ~450 nm and full-width-at-half-maximum (FWHM) of ~44 nm. Silica spheres with mean radius of 132 nm are initially diluted in de-ionized water to produce the optimized volume concentration of cv ~2%. 5 μL of diluted colloidal suspension mixed with sodium dedecyl sulfate (SDS) at a volume ratio of 10:1 is dispensed and dispersed uniformly across the sample by spin-coating. The SDS surfactant reduces water tension and prevents spheres from aggregating into clusters, thus forming monolayer of spheres. The ordered hexagonal pillar pattern is transferred to GaN by inductively coupled plasma (ICP) etching using Cl_2/He gas mixtures. The coil and platen powers are maintained at 500 W and 135 W while the chamber pressure is held constant at 5 mTorr. The spheres are then removed via sonication in deionized water. The etched sample is subsequently subjected to another NSL process. During spin-coating, the spheres spontaneously occupy locations at the triangular

a)Author to whom correspondence should be addressed. Electronic mail: hwchoi@hku.hk. Tel.: (852) 28592693. Fax: (852) 25598738.

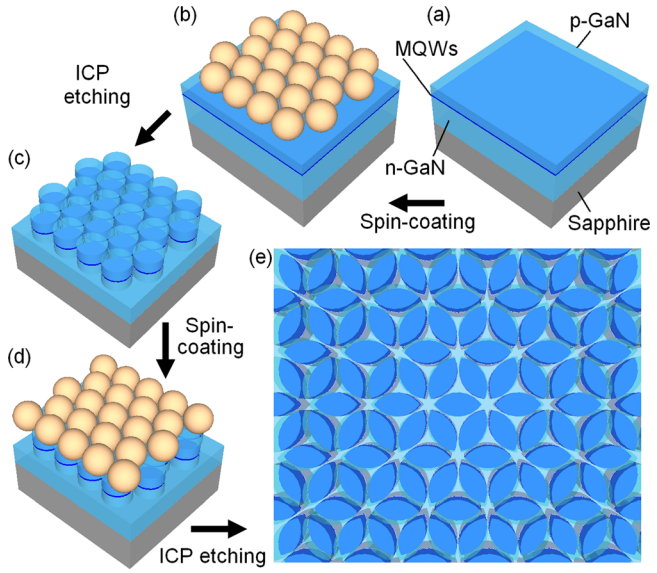

FIG. 1. Schematic diagram depicting the process flow; (a) the starting LED wafer; (b) silica spheres coated onto the wafer surface by spin-coating; (c) pattern transfer to GaN by ICP etching; (d) second monolayer of sphere array coated on top of pillar array; (e) clover-shaped pattern formed after ICP etching.

voids between adjacent pillars. After another dry etch process, the hexagonal CP clover-shaped PhC is formed. The surface morphologies of the resultant structures are imaged by field-emission scanning electron microscope (FE-SEM, Hitachi S-4800). The FE-SEM images in Figs. 2(a) and 2(b) show the hexagonal CP pillar array and the resultant clover-shaped structure, respectively. Time-integrated photoluminescence (PL) at room temperature is conducted to characterize the optical properties of PhC structure. The 349-nm excitation beam from a Spectra-Physics diode-pumped solid-state UV laser is focused onto the sample while the PL signal is fiber-collected to a spectrometer comprising of an Acton SP2500A 500 mm spectrograph and a Princeton Instrument

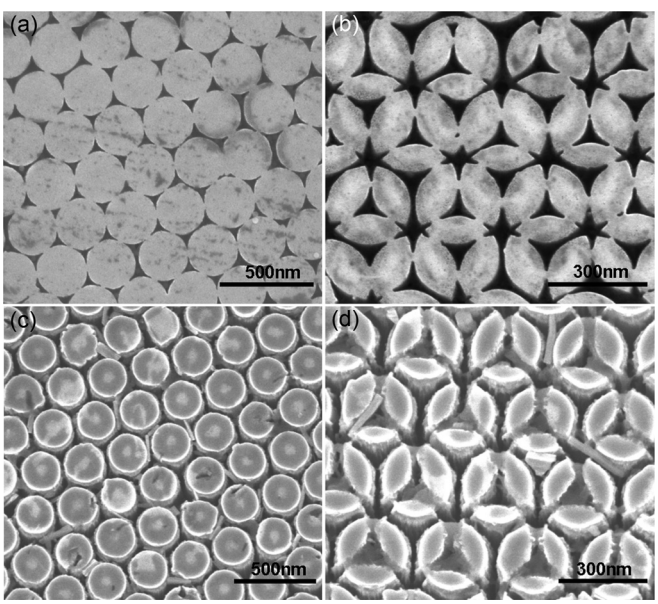

FIG. 2. FE-SEM images showing (a) the ordered hexagonal CP pillar array, (b) the CP clover-shaped PhC, (c) the NCP pillar array, and (d) the NCP clover-shaped PhC.

PIXIS open-electrode charge-coupled device. Time-resolved PL spectroscopy is conducted at room temperature using a pico-second laser (Passat Compiler) as an excitation source, whose wavelength is 266 nm with 8 ps pulse width and 100 Hz repetition rate. The PL signal is bandpass-filtered and collected via a 40 × UV objective, subsequently detected by a high-speed photodetector (Thorlabs SVC-FC, <150 ps rise time), whose electrical signal is read on a 4 GHz digital real-time sampling oscilloscope (Agilent DSO9404A, 85 ps rise time).

The band structures are computed by modified 3D-FDTD simulations to predict the PBG position of the clover-shaped PhC structure. The unit cell transformation technique is employed,[8] offering compatibility with any geometry, including the clover shaped structure of this study. Since the TE mode is dominant in emission of InGaN/GaN MQWs,[9] the TE band structures with varying ratios of pillar radius to pitch (r/a) are computed for both pillar and clover-shaped arrays, as plotted in Figs. 3(a) and 3(b), respectively. For the pillar arrays, the calculated bandgaps are discretely distributed throughout the plot. Although tuning of PBG can be achieved by modifying r/a ratios, the bandwidths are relatively narrow, varying from 8.98 nm at $r/a = 0.48$ (closed-packed) to 20.55 nm at $r/a = 0.41$, for effective coupling with QW emission. A detailed study on air-spaced pillar arrays has been reported in Ref. 7. On the other hand, the CP clover structure, with an r/a ratio of 0.48, possesses a PBG centered at 517.72 nm and a bandwidth of 12.18 nm. This PBG, being located at the green spectral region, does not coincide with the blue light emission from the InGaN/GaN MQWs of the wafers used in this study. However, the computed results also indicate that the PBG shifts gradually towards shorter wavelengths with decreasing r/a ratios, together with a broadening of the bandwidth to 53.87 nm at r/a of 0.41. To achieve a reduction of r/a, a selective dry etch step[7] can be inserted into the process flow to reduce the sphere radius r prior to pattern transfer onto GaN, ensuring that the centroids of the spheres do not shift so that the pitch a remains unchanged. Compared to the CP pillar array, spacing between pillars has been established with diameters of pillars reducing to ~230 nm, according to the FE-SEM image of Fig. 2(c). The sphere shrinkage process is repeated for the second sphere coating. The resultant NCP clover structure as illustrated in Fig. 2(d) has an r/a ratio of ~0.43 and is predicted to have a complete TE-PBG in the blue spectral region according to Fig. 3(b).

To experimentally determine the position of the PBG, an optical transmission measurement is conducted in the near-planar direction. The incident beam from a broadband solid-state plasma light source is focused onto the sample while the transmitted signal is measured by an optical spectrometer via fiber signal collection. Two pronounced dips with center wavelengths at 517.97 nm and 447.85 nm are clearly observed in Fig. 3(c) from the transmission spectra of the CP and NCP clover structures, corresponding to their respective bandgap positions. Transmission within the bandgap region does not fall to zero, attributed to out-coupling of light induced by random disorder within the PhCs. Such disorders originate from point and line defects, formed during the coating process, mainly arising from non-uniformities of

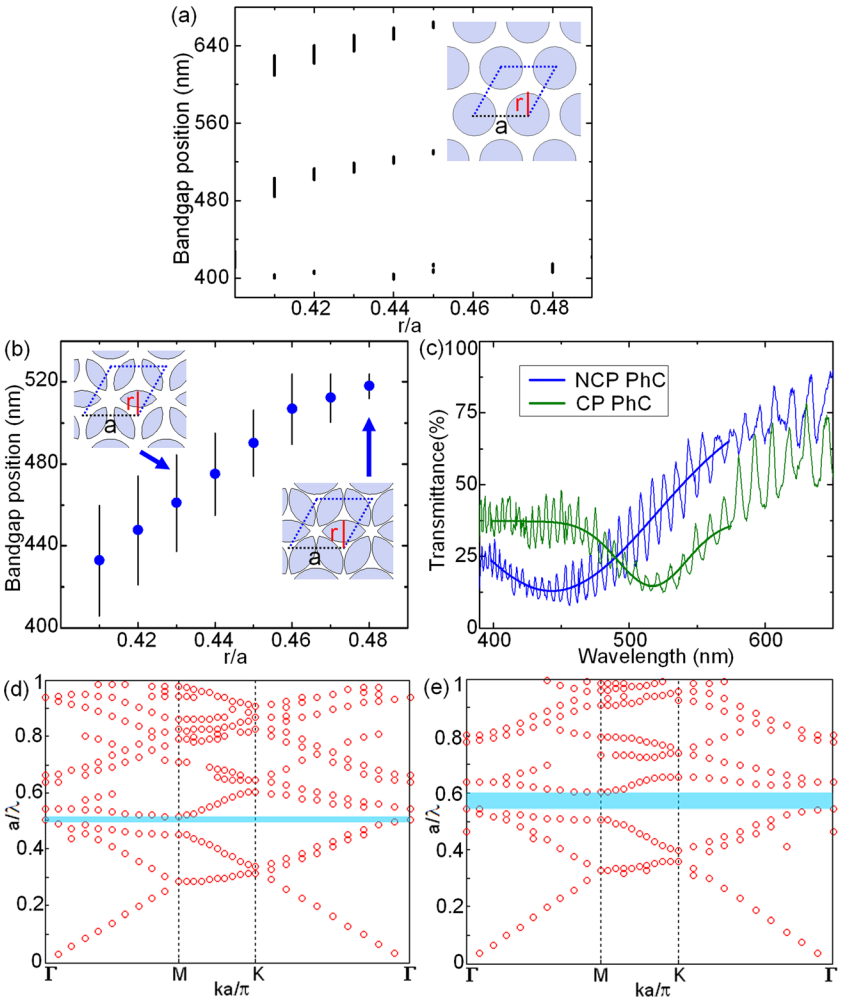

FIG. 3. Calculated bandgap as a function of r/a for (a) pillar arrays and (b) clover-shaped PhCs structures; (c) measured optical transmission spectrum from clover-shaped PhCs; simulated band diagram of (d) CP and (e) NCP clover-shaped structure, predicting PBG centered at ~517.72 nm and ~460.75 nm, respectively.

sphere dimensions and geometrical irregularities. At wavelengths beyond the range of frequencies covered by the PBG, relatively high transmission is maintained. The calculated band structure for the NCP clover structure as shown in Fig. 3(e) also confirms the presence of a PBG at the frequency range a/λ of 0.545–0.604, corresponding to wavelengths of 437.09–484.40 nm. Fig. 3(d) shows the narrower PBG located at the green light spectral region of 511.63–523.81 nm ($a/\lambda = 0.504$ to 0.516) for the CP array. The measured transmittance data correlate well with simulated results.

The optical enhancement of PhCs incorporation is assessed by conducting an angular-resolved PL measurement on the structures. The integrated PL intensity is collected at 1° intervals over an angular range of 90° at room temperature. Owing to high refractive index contrast at the GaN/air planar interface, a light beam striking the interface at incident angles beyond the critical angle determined by $sin^{-1}(n_{air}/n_{GaN}) \approx 24.6°$ will remain confined due to total internal reflection (TIR) and sequentially lost due to the reabsorption by the active layer, hence the rapid drop in PL intensity at angles beyond ~30° with respect to the normal, giving a narrow escape cone. According to the angular PL plot in Fig. 4(a), the FWHM of emission divergence increases from 128.72° in the unpatterned sample to 138.26° in the NCP PhC and 137.18° in the CP PhC; the clover-shaped PhCs can indeed expand the escape cone of light. Although the PBG position of the NCP clover structure does not correspond to emission spectrum, the nano-textured surface can still increase the probability of light escaping from the wafer via surface scattering, diminishing the losses caused by TIR. Compared to the unpatterned sample, a three-fold increase in PL intensity is observed from the NCP structure. The result indicates that proper design of a PhC is crucial for maximizing light extraction. The approach described here offers the capability of bandgap tuning, allowing optimal overlap between the PBG and emission wavelengths.

To further investigate the emission behavior of the PhCs, the PL spectra at each angle are measured; the individual normalized spectra are combined to generate angular-resolved emission patterns. For the as-grown sample, sharp Fabry-Perot interference fringes are observed as shown in Fig. 4(b), resulting from multiple reflections at the GaN/sapphire and the air/GaN interfaces, both with high refractive index contrasts. The NCP PhC structure maintains uniform emission intensity with faint fringes, as shown in Fig. 4(c), signifying that the optical confinement effect has been weakened. The improvement is attributed to Brillouin zone folding. Embedding such "weak" PhCs on top of the GaN wafer causes the dispersion curves of Bloch modes to become folded at the Brillouin zone boundary, allowing phase

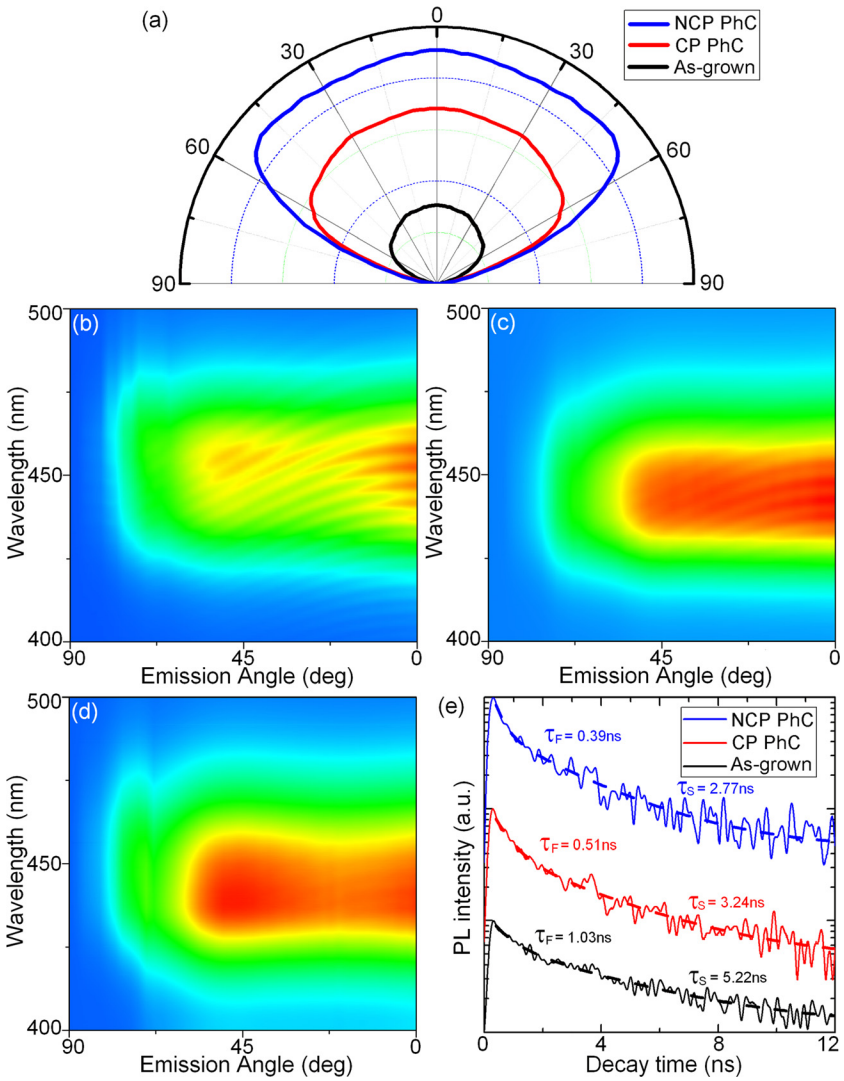

FIG. 4. (a) Angular PL plot showing integrated PL intensity versus azimuthal angle. Angular-resolved emission patterns for (b) as-grown, (c) CP, and (d) NCP clover-shaped PhCs. (e) Time-resolved PL decay profiles measured at room temperature. These decay profiles are fitted by double-exponential decay curves.

matching to the radiation modes that lie above this cut-off frequency.[10] The PhCs can further Bragg scatter the light emitted from the active region to avoid Fabry-Perot oscillations. The CP clover structure, on the other hand, acts as "strong" PhCs via a different mechanism—the PBG effect which significantly alters the properties of light propagation. The fringe-free spectrum obtained in Fig. 4(d) indicates that lateral propagation of Bloch guided modes is prohibited by the PBG; thereby light generated from MQWs will couple directly to radiation modes. Additionally, the spectrum from the clover structures exhibits a spectral blue-shift of ~6 nm compared to the as-grown, attributed to the partial strain relaxation of the MQW.

A time-resolved PL measurement is then carried out to examine the carrier dynamics. The PL decay rate can generally be expressed as the sum of the radiative and non-radiative recombination rates. The experimental data are fitted into two exponential decay profiles, as shown in Fig. 4(e). The fast decay component τ_F, which is strongly dependent upon thermally activated non-radiative recombinations at room temperature, is shortened to 0.39 ns and 0.51 ns for the NCP and CP PhCs, respectively, from 1.03 ns for the as-grown, attributed to higher surface recombination velocity as a result of increased etched sidewalls. On the other hand, the clover structures serve as optical nano-cavities which enhance carrier localization and reduce the quantum-confined stark effect, thereby accelerating the radiative recombination rates, as evident from the slow decay component τ_S. This is known as the Purcell effect, given by $1/\tau = F_p/\tau_o$ where F_p is the Purcell enhancement factor.[11]

In conclusion, the formation of CP and NCP clover-shaped PhCs has been demonstrated by dual-step NSL. The PBG determined from measured optical transmission spectra agrees well with the band structure as calculated by modified 3D-FDTD simulations. A three-fold enhancement in PL intensity is observed from the NCP clover-shaped PhCs, which has been optimized for the MQW emission band. Shortened PL decay lifetimes observed at room temperatures from PhCs structures suggest nano-cavities effects.

This work was supported by a GRF grant of the Research Grant Council of Hong Kong (Project HKU 7117/11 E).

[1]H. Matsubara, S. Yoshimoto, H. Saito, J. L. Yue, Y. Tanaka, and S. Noda, Science **319**, 445 (2008).
[2]J. C. Knight, Nature **424**, 847 (2003).
[3]C. F. Lai, J. Y. Chi, H. H. Yen, H. C. Kuo, C. H. Chao, H. T. Hsueh, J. F. T. Wang, C. Y. Huang, and W. Y. Yeh, Appl. Phys. Lett. **92**, 243118 (2008).
[4]T. N. Oder, J. Shakya, J. Y. Lin, and H. X. Jiang, Appl. Phys. Lett. **83**, 1231 (2003).

[5]D. H. Kim, C. O. Cho, Y. G. Roh, H. Jeon, Y. S. Park, J. Cho, J. S. Im, C. Sone, Y. Park, W. J. Choi, and Q. H. Park, Appl. Phys. Lett. **87**, 203508 (2005).
[6]W. Y. Fu, K. K. Y. Wong, and H. W. Choi, Appl. Phys. Lett. **95**, 133125 (2009).
[7]K. H. Li and H. W. Choi, J. Appl. Phys. **109**, 023107 (2011).
[8]Z. T. Ma and K. Ogusu, Opt. Commun. **282**, 1322 (2009).
[9]J. Shakya, K. Knabe, K. H. Kim, J. Li, J. Y. Lin, and H. X. Jiang, Appl. Phys. Lett. **86**, 091107 (2005).
[10]C. Wiesmann, K. Bergenek, N. Linder, and U. T. Schwarz, Laser Photonics Rev. **3**, 262 (2009).
[11]M. Boroditsky, R. Vrijen, T. F. Krauss, R. Coccioli, R. Bhat, and E. Yablonovitch, J. Lightwave Technol. **17**, 2096 (1999).